IIETA International Information and Engineering Technology Association
Advancing the World of Information and Engineering

Journal of New Materials for Electrochemical Systems
Vol.25, No.1, January 2022, pp. 38-45
Journal homepage: http://iieta.org/journals/jnmes

Investigation Photoluminescence Property of ZnO / PANI Nanocomposite Synthesized in [EtOHMIM$^+$] [HSO_4^-] Ionic Liquid and CTAB Surfactant

A. Benabdellah[1*], K. Negadi[2], Y. Chaker[2], B. Fettouhi[2], H. Belarbi[2], M. Hatti[3].

[1, 2]Synthesis and Catalysis Laboratory, University of Tiaret, Algeria.
[3] UDES, Solar Equipments Development Unit, Bou Ismail, Tipaza, Algeria.

Corresponding Author Email:abdelkader.benabdellah@univ-tiaret.dz

https://doi.org/10.14447/jnmes.v25i1.a06

Received: October 28, 2021
Accepted: January 05, 2022

Keywords:
ionic liquid, polyaniline, zinc oxide, nanocomposites, photoluminescence property.

ABSTRACT

In the present work, ZnO nanoparticles (NPs) were prepared using hydrothermal method with Trimethyl Ammonium Bromide (CTAB) as surfactant in 1- (hydroxyethyl)-3-methylimidazolium sulfate [EtOHMIM$^+$] [HSO_4^-] ionic liquid (IL). ZnO / PANI nanocomposite was prepared via in situ polymerization. The structures of the modified ZnO particles were characterized by X-ray diffraction, Raman spectroscopy and, scanning electron microscopy (SEM). The optical properties of (ZnO / PANI) nanocomposite were examined by photoluminescence (PL) analysis. XRD and, Raman analysis confirmed that pure ZnO (NPs) synthesized with (CTAB) in [EtOHMIM$^+$] [HSO_4^-] IL were formed. The addition of (CTAB) and [EtOHMIM$^+$] [HSO_4^-] IL does not change the ZnO phase but reduces the particle size of ZnO and converts shallow defects to deep defects. The SEM images of the ZnO / PANI nanocomposite showed the formation of hexagonal wurtzite ZnO (NPs) embedded in polyaniline matrix. The PL intensity of the ZnO / PANI nanocomposite is improved as compared to pure ZnO (NPs). This indicates that [EtOHMIM$^+$] [HSO_4^-] IL may be acting as a dye, since it is constituted by an organic part, [EtOHMIM$^+$]. This good performance indicates that the synthesised nanocompsite is promising material as photoanode in solar cells.

1. INTRODUCTION

In recent years, the development of inorganic / polymer hybrid materials on nanometer scale has been receiving significant attention due to a wide range of potential applications in optoelectronic devices [1-3] and in field effect transistors [4]. Semiconducting zinc oxide (ZnO) is attracting a lot of attention due to its unique properties such as direct wide band gap (3.37 eV) and large exciton binding energy (60 meV) at room temperature [5]. Due to these properties it has been studied extensively for making optical and electronic devices [6, 7]. Nanostructured ZnO can be synthesized by various methods such as physical, chemical, electrochemical, deposition techniques [8-11]. Many studies on the preparation of polymer nanocomposites have been reported in the quest to develop new advanced materials with improved mechanical, electrical, optical and catalytic properties or to improve conduction mechanism in electronic devices. Polyaniline (PANI) is the most studied polymer because of its relative ease in preparation, good environmental stability [12, 13] and tunable conductivity. The preparation of PANI composites with various oxide materials such as Fe_3O_4 / PANI, MnO_2 / PANI, TiO_2 / PANI and ZrO2 / PANI [14, 15], as well as preparation and characterization of ZnO / PANI composites have been published [16-18]. Due to these properties it has been studied extensively for making optical and electronic devices [19-21]. CetylTrimethyl Ammonium Bromide (CTAB) a cationic surfactant is the most commonly used stabilizing agent in controlling the shape and size of NPs which can play a modified part in the process of organic synthesis of materials [22]. Ionic liquids (ILs) exhibit high chemical and thermal stability, non-volatility, non-flammability, high ionic conductivity, and a wide electrochemical window [23, 24]. Due to these characteristics, they are proposed to improve properties in different fields such as batteries [25], fuel cells [26] and supercapacitors [27]. In this paper, we report the preparation and characterization of ZnO (NPs) synthesized with CetylTrimethyl Ammonium Bromide (CTAB) in 1-(hydroxyethyl)-3-methylimidazolium sulfate [EtOHMIM$^+$] [HSO_4^-] IL. The structural, morphological optical and photoluminescence properties of ZnO / PANI nanocomposite were investigated using XRD, Raman, SEM and PL analysis. ZnO / PANI nanocomposite so formed resulted in an altogether different optical and structural property. Raman spectroscopy and photoluminescence study were employed as tools to investigate the hybrid effect between ZnO NPs synthesized with CTAB in [EtOHMIM$^+$] [HSO_4^-] IL and PANI.

2. REAGENTS AND INSTRUMENTS

2.1. Reagents and materials

Aniline (99.5%) and zinc acetate dihydrate (99.5%) were procured from Sigma Aldrich.Aniline was distilled prior to use. All supplementary chemicals (Ammonium peroxydisulfate, NaOH, HCl, acetone, ethanol) (99%), Methanol (99.5%), Tetrahydrofurane (THF)and

Cetyltrimethylammonium bromide (CTAB) (99%) were all obtained from Merck.All thechemicals and reagents were used as received without furtherpurification.

2.2 Instruments

X-ray powder diffraction (XRD) analysis was conducted on a Rigaku Smart Lab operated at 40 kV and 35 mA using Cu Kα radiation (λ=1.54059 ˚A). The Raman instrument was coupled to a standard Olympus microscope and a collection optics system. The excitation source was a 514.5nm Ar+ laser line. The optical power at the sample position was maintained at 5mW. The scattered light was collected in the backscattering configuration and the spectra were recorded at a resolution of 2.0 cm^{-1}. Scanning electron microscopy (SEM Model: JEOL JSM 6360) operating at 20 kV.

3. EXPERIMENTAL PROCEDURES

3.1. Preparation of ZnO NPs + CTAB / [EtOHMIM+] [HSO4-] IL

Preparation of zinc oxide nanoparticles were performed using 0.1M of zinc acetate dihydrate (solution-A), sodium hydroxide (2M) (solution-B) and N-Cetyl-N,N,N-Trimethylammonium bromide (CTAB) (0.1M)disolved in double distilled water.90 ml of double distilled water was taken in a conical flask and 5 ml of solution-A was added to it, followed by the addition of 5 ml of solutionB. The mixture was heated to 70°C with vigorous stirring for 15 min.The reaction was carried in presence of CTAB as surfactant. The precipitates were separated, washed with double distilled water and acetone five times for 1hour using centrifugation at 3500 rpm to remove the non reacted materials. Zinc hydroxide can be easily converted to ZnO (NPs) by drying.So, the product dried at 65°C overnight.Finally, the product was crashed using mortar and pestle to produce fine powder. The preparation and characterization of 1-(hydroxyethyl)-3-methylimidazolium sulfate [EtOHMIM$^+$] [HSO_4^-] IL was carried out by the procedure described in the literature [28]. Distilled before use at 70°C.The desired amount of [EtOHMIM$^+$] [HSO_4^-] IL (50 mM) was added to the Zn (NPs) + CTAB. The solution was stirred for 10 min,and then the reaction mixture was sealed into a glass tube and heated at 80°C (chosen so that the temperature does not exceed the boiling point of the components) for 48 h to ensure the completeness of reaction. Finally, the product Zn (NPs) + CTAB / [EtOHMIM$^+$] [HSO_4^-] IL was separated by centrifugation, washed with absolute ethanol and water several times and sonicated between washes, followed by dryingfor1hat80°C.

3.1. Synthesis of ZnO / PANI Nanocomposite

5g of ZnO (NPs) synthesized with CTAB in [EtOHMIM$^+$] [HSO_4^-] IL were dispersed in 0.05M HCl solution in a three-neck round-bottomed flask which was fitted with ultrasonic vibration device for one hour. Then 2 mL of aniline monomer was added to the above mixture. The mixtures were stirred with magnetic stirrers in ice water baths (0°C- 5°C) for 4 h to get a uniform suspension of the nanocomposite. Under the protection with nitrogen gas, 5g of ammonium peroxydisulfate (APS) dissolved in 2M HCl solution which serves as an oxidant, was added drop wise into the above mixture. ZnO / PANI nanocomposite was washed with distilled water, methanol and acetone, and then dried in a vacuum for 12 hours at 5°C.

4. RESULTS AND DISCUSSION

4.1. XRD analysis

The XRD technique was used to examine the crystal phases and crystallinity of thesynthesized ZnO (NPs) with CTAB in [EtOHMIM$^+$] [HSO_4^-] IL and ZnO / PANI Nanocomposite as shown in Fig.1.It is seen inthe XRD patterns curves that all the peaks of ZnO (NPs) are obtained, which correspond to the hexagonal wurtzite structure phase pure ZnO (NPs) , appearing well-defined diffraction reflections at different angles 31.6°, 34.3°, 36.2°, 47.5°, 58.6°, 62.8°, 64.3°, 68.1° and 69.3° corresponding to the (100), (002), (101), (102), (110), (103), (200), (112), and (201) lattice planes respectively.The observed diffraction reflections are well matched with the reported literature [29].

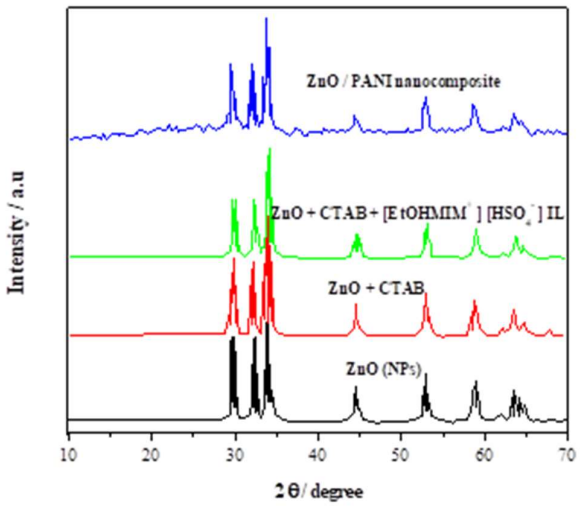

Figure 1. XRD pattern of ZnO (NPs), ZnO + CTAB, ZnO + CTAB / [EtOHMIM$^+$] [HSO_4^-] and ZnO / PANI Nanocomposite

No other reflection related with any impurity was detected in the pattern up to the detection limit of the XRD diffractometer, which further confirmed that the synthesized products were pure ZnO (NPs), without any significant impurity.It can be seen that the addition of CTAB and [EtOHMIM$^+$] [HSO_4^-] IL do not alter the crystal phase of ZnO (NPs). From the results, we can observe that insertion of the CTAB did not significantly change the lattice parameters of ZnO (NPs). However, a decrease in the average size of the crystallite can be observed with insertion of [EtOHMIM$^+$] [HSO_4^-] IL. In the case of ZnO / PANI Nanocomposite, XRD spectra show peaks for both PANI and ZnO (NPs).Further, thepeaks are slightly shifted towards higher 2θ value and the intensity is enhanced on ZnO (NPs) incorporation. Shift in peaks and change in intensity of the peaks may be a consequence of the change in bond length and bond stretching in the composite. This indicates that the in-

situ formed ZnO (NPs) are well incorporated into the polymer matrix [30].

4.2. Raman spectroscopy analysis

Raman spectroscopy was carried out to analyze any changes in the lattice vibrations of the ZnO (NPs) nanostructure upon addition of CTAB and [EtOHMIM$^+$] [HSO_4^-] IL. Fig.2 displays the Raman spectra of wurtzite ZnO (NPs)synthesized with CTAB in [EtOHMIM$^+$] [HSO_4^-] IL.

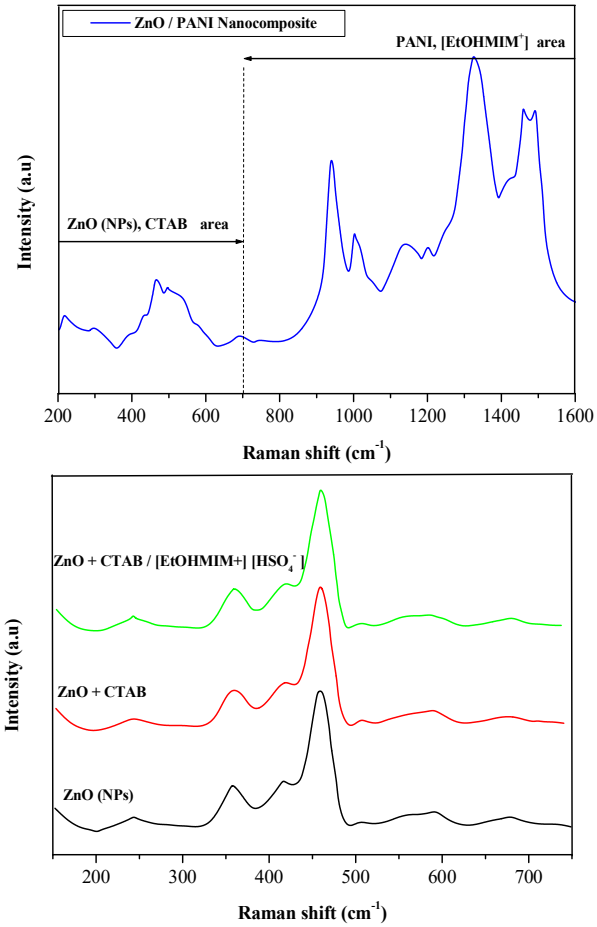

Figure 2. Raman spectra of ZnO (NPs), ZnO + CTAB, ZnO + CTAB / [EtOHMIM$^+$] [HSO_4^-] and ZnO / PANI Nanocomposite

The modes A1 and E1 are split into transverse (TO) and longitudinal optical (LO) phonons, while the E2 modes are non-polar.The A1 and E1 modes are Raman and infrared active, the E2 modes are only Raman active, and the B1 modes are Raman and infrared inactive [31].

ZnO / PANI nanocomposite presents optical phonons at the Γ point of the Brillouinzone corresponding to the irreducible representation, in equation (1) :

$$\Gamma_{opt} = A_1 + E_1 + 2E_2 + 2B_1 \qquad (1)$$

The zone center optical mode frequencies lie between about 100 cm^{-1} and 700 cm^{-1}. The group E1 (LO), A1 (LO), and B1 (high) modes occurs in the highest frequency range, 570 cm^{-1} to 620 cm^{-1}.The groups E2 (high), E1(TO) and A1 (TO) appear between 350 cm^{-1} and 450 cm^{-1}. The E2 (low) and the B1 (low) modes appear in the frequencies 100 cm^{-1} and 250 cm^{-1},respectively[32]. Fig.2 shows a strong and dominant peak at 464 cm^{-1} for pure ZnO (NPs) and ZnO +CTAB / [EtOHMIM$^+$] [HSO_4^-] IL samples, attributed to the lattice vibration of oxygen atoms and mostly assigned to E2 (high) phonon mode [33]. This peak at 101 cm^{-1},E2 (low) is a characteristic of scattering peaks of the Raman active dominant modes of wurtzite hexagonal ZnO (NPs), indicating the excellent quality of the crystal [34,35].The peak at 420 cm^{-1} is attributed to the A1 (TO) mode [32], while those at 223 and 365 cm^{-1}can be assigned to the acoustic phonon overtone and optical phonon overtone with the A1 symmetry [34]. The Raman mode at 570 cm^{-1} corresponds to the E1 (LO) mode of ZnO (NPs)[36]. The peak at 678 cm^{-1} corresponds to additional vibrational modes associated with defects [37]. It is possible to observe that the addition of CTAB and [EtOHMIM$^+$] [HSO_4^-] IL does not change the lattice vibrations of the ZnO nanostructure.In the case of ZnO/PANI nanocomposite the Raman spectrahas a peak at 1489 cm^{-1} corresponding to C=N stretching enhances whereas peak at 1600 cm^{-1} in the composite diminishes which signifies that semiquinones disappears and quinones peak starts (1489 cm^{-1}) arising confirming an increase in the linkages of ZnO with PANI. Also, stretching vibrations because of the C-H of benzenoid rings at 1192 cm^{-1} shift to 1189 cm^{-1} and a peak at 1166 cm^{-1} due to the C-H bending of quinoids emerges.

4.3. Morphological studies

Typical SEM images of ZnO (NPs), ZnO+CTAB, ZnO+CTAB / [EtOHMIM$^+$] [HSO_4^-] IL and ZnO / PANIare shown in Fig.3. (A, B, C, D) respectively.

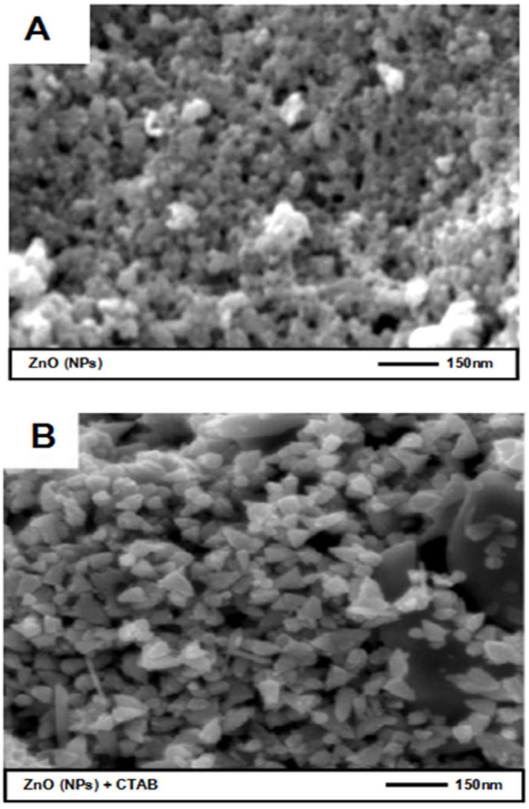

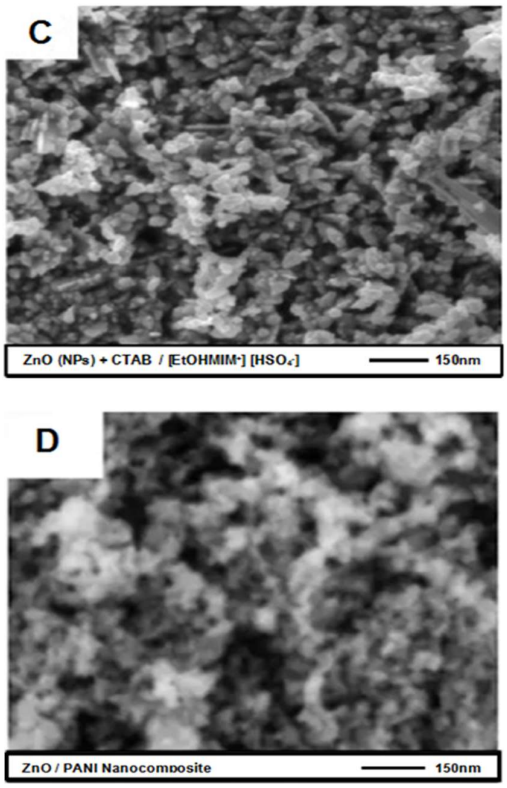

Figure 3. SEM of (A)- ZnO (NPs), (B)- ZnO+CTAB, (C)- ZnO+CTAB/ [EtOHMIM+] [HSO4-] and (D)- ZnO / PANI Nanocomposite

The ZnO (NPs) (Fig.3.A)are reasonably uniform in size, and the morphology of the ZnO (NPs) takes on pseudo-spherical shape [37]. The average size of the ZnO (NPs) is approximately 60 nm, which is consistent with the crystallite size estimated from the XRD analysis. The SEM micrograph of ZnO (NPs) prepared with CTAB(Fig.3.B) indicates the presence of the size of particles varies in a range between few tens of nanometres to hundreds of nanometres. The images reveal that the produced nanoparticles are almost homogeneous in shape.When the [EtOHMIM^{+}] [HSO_4^-] IL was added to the ZnO (NPs) + CTAB (Fig.3.C), no changes occurred in the morphology, however the nanostructures are observed to coalesce. [EtOHMIM^{+}] [HSO_4^-] IL caused changes in the ZnO (NPS) size, the particle size and thickness of the particles.Upon the addition of [EtOHMIM^{+}] [HSO_4^-] IL the average particle size decreased to 2µm and the thickness to 0.04µm for the ZnO (NPs). This decrease in particle size upon the addition of ionic liquid has also been reported in the literature [38, 39]. Surface images of PANI/ZnO nanocomposite indicatethat the morphology of PANI has changed by the introduction of ZnO (NPs), as depicted in Fig.3.D. The diameter of PANI is approximately 100nm, with irregular road-like morphology. The introduction of ZnO (NPs) can reduce PANI size. This agglomeration is caused by hydrogen bonds that occur due to the interaction between ZnO and N-H groups or coordination bonds [39-40]. The SEM image helped us to conclude that the introduction of ZnO (NPs) has a strong effect on the morphology of PANI, since PANI has various structures such as granules, nanofiber, nanotubes, nanosphere, microspheres and flake [41].

4.4. Band gap energy measurements

Figure 4 shows the band gap values for ZnO (NPs), ZnO+CTAB, ZnO+CTAB / [EtOHMIM^{+}] [HSO_4^-] IL and ZnO / PANInanocomposite to be 3.15, 3.07, 3.14, and 3.02 eV, respectively.

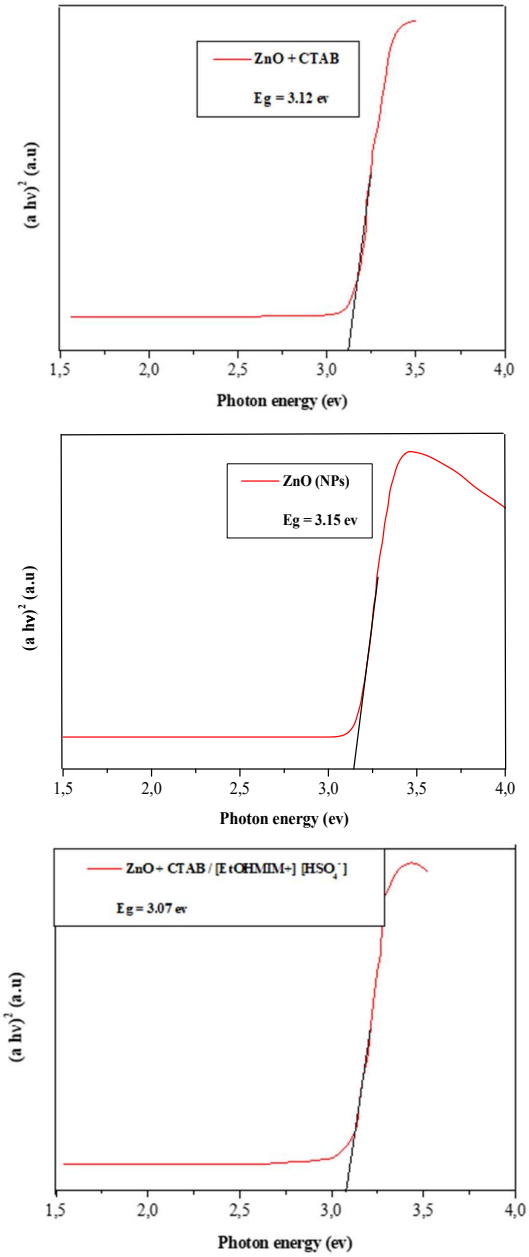

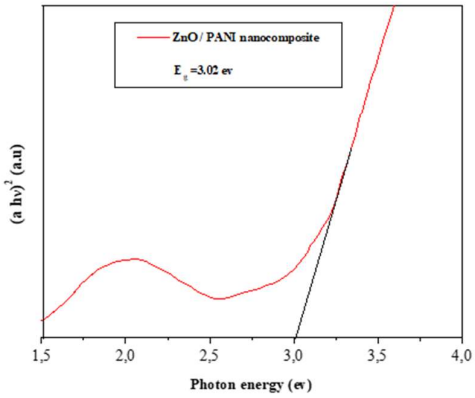

Figure 4. Band gap energy of ZnO (NPs), ZnO + CTAB, ZnO + CTAB / [EtOHMIM$^+$] [HSO_4^-] and ZnO / PANI Nanocomposite

The band gap energies (Eg, eV) of the samples have been calculated, in order to investigate the effect of the[EtOHMIM$^+$] [HSO_4^-]IL on the optical properties of ZnO (NPs) and ZnO / PANI nanocomposite.The Eg of the samples was calculated by the Kubelka and Munk method [41], using the equation:

$$\alpha h\nu = K\left(h\nu - E_g\right)^n \qquad (2)$$

Where $h\nu$ the energy of the incident light and K is a constant. The intercept of the linear part of αhν vs hν curve on the x-axis gives the value of Eg. The band gap energy values found for ZnO (NPs), ZnO+ CTAB, ZnO+ CTAB / [EtOHMIM$^+$] [HSO_4^-] IL and ZnO / PANI nanocomposite samples were very similar, in agreement with a

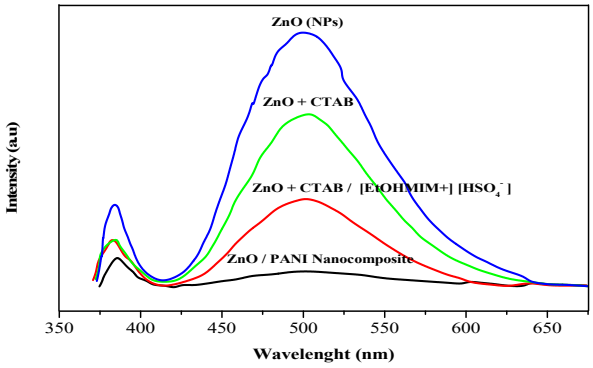

Figure 5. Photoluminescence spectra of ZnO (NPs), ZnO + CTAB, ZnO + CTAB/ [EtOHMIM$^+$] [HSO_4^-] and ZnO / PANI Nanocomposite

The PL spectrum of pure ZnO (NPs) presents a broad band with the emission maximum centered at λ=619.1 nm. When the ZnO (NPs) was doped with CTAB and [EtOHMIM$^+$] [HSO_4^-]IL, the spectra had emission maxima centered at λ=648 nm and λ=638 nm for ZnO + CTAB and ZnO + CTAB/[EtOHMIM$^+$] [HSO_4^-] ILrespectively.PL properties and contribution of each individual peak observed in the samplescan be attributed to the recombination of isolated electrons in the vacancies of ionized oxygen (V0) with photogenerated holes [44]. The spectra of ZnO + CTAB and ZnO + CTAB /[EtOHMIM$^+$] [HSO_4^-] IL components are crystallographic profile similar to those indicated by XRD results. The theoretical band gap for ZnO powder is 3.3 eV [7, 40]. Therefore, these results show that the ZnO NPs synthesized in this work present defects, which introduce intermediate levels between ZnO (NPs) between the valence band and the conduction band. The band gap of ZnO / PANI increases nearly exponentially, so we can claim that ZnO (NPs) synthesised in [EtOHMIM$^+$] [HSO_4^-] IL leads to tune the band gap of PANI. That is, the particle size of ZnO NPs decreases in the presence of [EtOHMIM$^+$] [HSO_4^-] IL. One of the reasons for such behaviour in the composites lies in the fact that the in-situ formed ZnO (NPs) which is known to have negatively charged surface has more affinity towards PANI which is known to possess positively charged surface. For that reason there is a decrease in overlap of p-orbitals present in carbon atoms of the PANI molecules upon ZnO incorporation. This correlates with conventional phenomena of quantum confinement in nanomaterials which says that smaller crystallites have larger band gap. As the particle size of a material decreases, the availability of active sites on the surface increases, another well known phenomena in nanomaterials to have larger surface/volume ratio in lowering the dimension.

4.5. Photoluminescence (PL) studies

Fig. 5 shows the PL spectra of ZnO (NPs), ZnO + CTAB, ZnO + CTAB /[EtOHMIM$^+$] [HSO_4^-]IL and ZnO/PANInanocomposite using an excitation laser with λ=350 nm at room temperature. The profile of the PL emission band is typical of a multiphotonprocess, which involves different states within the band gap [42-43].For the bare ZnO NPs, a weak ultraviolet peak at 387 nm and a strong emission at 500 nm are observed.
located at the same energy values as ZnO (NPs). Since singled charged oxygen vacancies are responsible for green emission, its reduction can be related with the decrease in the number of these vacancies [45]. Thus, the addition of ionic liquid in the material decreases the number of oxygen vacancies and, as a consequence, singled charged oxygen vacancies, but the number of doubly charged oxygen vacancies remains almost unchanged. PL of ZnO / PANI nanocomposite do not exhibit an emission at λmax = 350 nm.When ZnO (NPS) modified by CTAB and [EtOHMIM$^+$] [HSO_4^-] IL areintroduced in the polyaniline matrix, it is observed that the intensity of green emission falls while an enhancement in band gap emission is observed.It is assumed that UV emission efficiency improved because of the passivation of green emission centers [34].

5. CONCLUSION

In this work the preparation and characterization of ZnO (NPs) had been synthesized with (CTAB) in [EtOHMIM$^+$] [HSO_4^-] ionic liquidby a simple, cost effective technique. XRD and, Raman analyses confirmedthat pure ZnO (NPs)synthesized with CTAB in [EtOHMIM$^+$] [HSO_4^-] IL were formed. The crystallite size for ZnO (NPs) was found to be 30nm.The results obtained from SEM studies exactly matched with XRD,which confirmed the formation of ZnO (NPs). ZnO NPs crystal phase is not altered with the addition of CTAB and [EtOHMIM$^+$] [HSO_4^-] IL, but a decrease in the average size of the crystallite can be observed.XRD and

Raman of ZnO / PANI nanocomposite revealed that PANI undergoes interaction with ZnO (NPs). SEM micrograph shows the uniform distribution of ZnO (NPs) in ZnO / PANI nanocomposite.Photoluminescence (PL)measurements confirmed the sensitization of ZnO NPswith CTAB in [$EtOHMIM^+$] [HSO_4^-] IL, indicating that the ionic liquid acts as an efficient dye on the ZnO / PANI.

ACKNOWLEDGEMENTS

This work is partially of a research project supported by CNEPRU (code: B00L01UN140120150002) of research direction (Algerian Ministry of Higher Education and Scientific Research). The authors also gratefully acknowledge the helpful comments and suggestions of the reviewers, which have improved the presentation.

REFERENCES

[1] A. Benabdellah, H. Belarbi, H. Ilikti, T. Benabdallah, M Hatti, Magnetic properties of polyaniline/ZFe2O4 nanocomposites synthesized in CTAB as surfactant and Ionic Liquid, Tenside Surfactants Detergents,52, (2015) 484-492. https://doi.org /10.31 39/113.110401.

[2] Xinjie Tao, Yongli Li, Yuechan Li, Dongya Sun, AnXie. Electroluminescent Polymer Materials and Their Applications,J. New Mat. Electrochem. Systems,6(2021)231-238. https://doi.org/10.18280/acsm.450306

[3] X.H. Li, C.L. Shao, Y.C. Liu, X.Y. Chu, C.H. Wang, B.X. Zhang, Photoluminescence properties of highly dispersed ZnO quantum dots in polyvinyl pyrrolidonenanotubes prepared by a single capillary electrospinning, The Journal of Chemical Physics, 129, Issue 11, (2008) 113-118, https://doi.org/10.1063/1.2977969

[4] D.C. Olson, J. Piris, R.T. Collins, S.E. Shaheen, D.S. Ginley, Hybrid photovoltaic devices of polymer and ZnO nanofiber composites, Thin Solid Films, 496, Issue 1, (2006) 26-29. https://doi.org/10.1016/j.tsf.2005.08.179.

[5] P. Yang, H. Yan, S. Mao, R. Russo, J. Johnson, R. Saykally, N. Morris, J. Pham, R. He, H.J. Choi, Controlled growth of Zinc oxide nanowires and their optical properties, Advanced Functional Materials, 12 (5), (2002) 323-331. https://doi.org/10.1002/1616-3028 (20020517) 12:53.0.CO;2-G.

[6] L. Xu, G. Zhenga,Y. Liu, J. Su, W. Kuang, W. Rao, the optical properties of Ag/ZnO nanocomposite thin films with different thickness, Optik journal, 147, (2017) 6-13. https://doi.org/10.1016/j.ijleo.2017.08.078

[7] H. Zhang, Z. Jia, Application of porous silicon microcavity to enhance photoluminescence of ZnO/PS nanocomposites in UV light emission, Optik journal, 130 (2017) 1183-1190. https://doi.org/10.1016/j.ijleo.2016.11.131.

[8] Asmaa H. Dhiaa*, Marwa A. Salih, Hayder A. Al-Yousefi. Effect of ZnO Nanoparticles on the Thermo-Physical Properties and Heat Transfer of Nano-Fluid Flows,J.New Mat. Electrochem. Systems, 38 (2020) 715-721. https://doi.org/10.18280/ijht.380316.

[9] J.K. Salem, Synthesis of disk-like and flower-like ZnO nanostructures by sodium dodecyl sulfate-assisted non-basic solution process,Tenside Surfactants Detergents,48, Issue 3, (2011) 206-209. https://doi.org/10.3139/ 113.110123.

[10] B. Rahal, B. Boudine, A. R. Khantoul, M. Sebais, O. Halimi, Colloidal synthesis of nanostructured pure ZnO and Cd doped ZnO thin films and their characterization, Optik journal, 127 (17), (2016) 6943-6951. https://doi.org/10.1016/j.ijleo.2016.05.006

[11] [11] X. Shen, G. Zhang, Y. Yang, S. Yu, Template-free hydrothermal synthesis of tubular ZnO clusters and rods,International Journal of Materials Research, 102, Issue 2, (2011) 187-193. https://doi.org/10.3139/146.110458.

[12] [12] S.H. Kim, J. Jang, J.Y. Lee, High efficiency phosphorescent organic light-emitting diodes using carbazole-type triplet exciton blocking layer, Applied Physics Letters, 90, Issue 22, (2007) 505-509. https://doi.org/10.1063/1.2742788.

[13] G. Gustafsson, Y. Cao, G. M. Treacy, F. Klavetter, N. Colaneri, A. Heeger, Flexible light-emitting diodes made from soluble conducting polymers, Nature, 357, (1992) 477-479. https://doi.org/10.1038/357477a0.

[14] Xochitl D. Benetton*, S.G. Navarro-Ávila, C. Carrera-Figueiras. Electrochemical evaluation of Ti/TiO2-polyaniline Anodes for Microbial Fuel Cells using Hypersaline Microbial Consortia for Synthetic-wastewater Treatment, J. New Mat. Electrochem. Systems, 13(2010) 1-6. https://doi.org/10.14447/jnmes.v13i1.184.

[15] A.G. Yavuz, A. Gok, Preparation of TiO2/PANI composites in the presence of surfactants and investigation of electrical properties, Synthetic Metals,157, Issue 4-5, (2007) 235–242. https://doi.org/10.1016/j.synthmet.2007.03.001.

[16] B. Yuan, Y. Xia, M. Li, Q. Zhu, Synthesis of ZnO nanomaterials with different morphologies by hydrothermal method,International Journal of Materials Research, 109, Issue 10, (2018) 910-915. https://doi.org/10.3139/146.111696.

[17] O. Saiah, A. Hachemaoui, A. Yahiaoui, Synthesis of a conducting nanocomposite by intercalative copolymerisation of furan and aniline in montmorillonite, International Polymer Processing, 32, Issue 4, (2017) 515-518. https://doi.org/10.3139/217.3419.

[18] H. Zhang, R. Zong, Y. Zhu, Photocorrosion inhibition and photoactivity enhancement for Zinc oxide via Hybridization with monolayer polyaniline, The Journal of Physical Chemistry C, 113, (2009) 4605-4611https://doi.org/10.1021/jp810748u. [19] S. L. Patil, M. A. Chougule, S.G. Pawar, S. Sen, V. B. Patil, Effect of camphor sulfonic acid doping on structural, morphological, optical and electrical transport properties on polyaniline-ZnO nanocomposites. Soft Nanoscience Letters, 2, (2012) 8. https://doi.org/10.4236/snl.2012.23009

[19] W.I. Park, G.C. Yi, M. Kim, S. J. Pennycook, ZnO nanoneedles grown vertically on Si substrates by non-catalytic vapor-phase epitaxy, Advanced Materials, 14,

Issue 24, (2002) 1841-1843. https://doi.org/10.1002/adma.200290015.

[20] L. Vayssieres, K. Keis, A. Hagfeldt, S. Lindquist, Three-dimensional array of highly oriented crystalline ZnO microtubes, Chemistry of Materials, 13, Issue 12, (2001) 4395-4398.https://doi.org/10.1021/cm011160s.

[21] D. Sridevi, K. V. Rajendran, Influence of surfactants on the morphologies of CdSnanorods, Tenside Surfactants Detergents, 48, Issue 3, (2011) 197-199. https://doi.org /10.3139/113.11 0121.

[22] Suresha K. Mahadeva | JyotiNayak | Jaehwan Kim. Structure, Tensile and ElectromechanicalProperties of 1-Butyl-3-Methylimidazolium bis (trifluoromethylsulfonyl)imide Incorporated Cellulose, J. New Mat. Electrochem. Systems, 13(2010) 113-117.https://doi.org/10.14447/jnmes.v13i2.178.

[23] W. Kunz, K. Häckl, The hype with ionic liquids as solvents, Chemical Physics Letters, 661 (2016) 6–12. https://doi.org/10.1016/j.cplett.2016.07.044.

[24] A. Eftekhari, Y. Liu, P. Chen, Different roles of ionic liquids in lithium batteries, Journal of PowerSources, 334, (2016) 221–239. https://doi.org /10.1016/ j.jpowsour .2016.10.025

[25] M. Díaz, A. Ortiz, I. Ortiz, Progress in the use of ionic liquids as electrolyte membranes in fuel cells, Journal of Membrane Science, 469, (2014) 379–396. https://doi.org/10.1016/ j.memsci.2014.06.033.

[26] J. Li, J. Tang, J. Yuan, K. Zhang, Q. Shao, Y. Sun, L.C. Qin, Interactions between graphene and ionic liquid electrolyte in supercapacitors, ElectrochimicaActa, 197, (2016) 84–91. https://doi.org/10.1016/j.electacta.2016.03.036.

[27] Y. Chaker, H. Ilikti, M. Debdab, T. Moumene, H. Belarbi, A. Wadouachi, O. Abbas,B. Khelifa, S. Bresson, Synthesis and characterization of 1-(hydroxyethyl)-3-methyl-imidazolium sulfate and chloride ionic liquids,Journal of Molecular Structure, 1113, (2016) 182-190.https://doi.org/10 .10 16 / j. molstruc.2016.02.017.

[28] K. Ding, H. Jia, S. Wei, Z. Guo, Electrocatalysis of sandwich-structured Pd/Polypyrrole/Pd composites toward formic acid oxidation, Industrial & Engineering Chemistry, 50, Issue 11, (2011) 7077-7082. https://doi.org/10.1021/ie102392n.

[29] Y. He, A novel emulsion route to sub-micrometer polyaniline/nano-ZnO composite fibers, Applied Surface Science, 249, Issues 1-4, (2005) 1–6.https://doi.org /10.1016/j.apsusc.2004.11.061.

[30] C. Bundesmann, N. Ashkenov, M. Schubert, D. Spemann, T. Butz, E. M. Kaidashev, M. Lorenz, M. Grundmann, Raman scattering in ZnO thin films doped with Fe, Sb, Al, Ga, and Li , Applied Physics Letters , 83, Issue 10, (2003) 74. https://doi.org/10.1063/1.1609251

[31] N. Roy, A. Chowdhury, T. Paul, A. Roy, Morphological, optical, and Raman characteristics of ZnO nanoflowers on ZnO-seeded Si substrates synthesized by chemical method, Journal of Nanoscience and Nanotechnology, 16, 9, (2016) 9738–9745. https://doi.org/10.1166/ jnn.2016.12355.

[32] R. Cusco, E. Alarcon-Llado, J. Ibanez, L. Artus, J. Jimenez, B. Wang, M.J. Callahan, Temperature dependence of Raman scattering in ZnO, Phys Rev B, 75, Issue 16, (2007) 165-202.https://doi.org/10.1103/PhysRevB.75.165202.

[33] R. Zhang, P.G. Yin, N. Wang, L. Guo, Photoluminescence and Raman scattering of ZnO nanorods, Solid State Science, 11, Issue 4, (2009) 865–869.https://doi.org /10.1016/j.2008.10.016.

[34] J. Sann, J. Stehr, A. Hofstaetter, D.M. Hoffmann, A. Neumann, M. Lerch, U. Haboek, A. Hoffmann, C. Thomsen, Zn interstitial related donors in ammonia-treated ZnO powders, Phys. Rev B, 76, (2007) 195-203. https://doi.org /10.1103/PhysRevB.76.195203.

[35] D.N. Montenegro, V. Hortelano, O. Martínez,.Martínez-Tomas, M.C. Sallet, V. Munoz-Sanjosé, V. Jimenez, J, Non-radiative recombination centres in catalyst free ZnO nanorods grown by atmospheric-metal organic chemical vapour deposition, J. Phys. D: Appl. Phys, 46, (2013) 235-302. https://doi.org/10.1088/0022-3727/46/23/235302 (4pp).

[36] B. Yuan, Y. Xia, M. Li, Q. Zhu, Synthesis of ZnO nanomaterials with different morphologies by hydrothermal method, International Journal of Materials Research, 109, Issue 10, (2019) 910-915. https://doi.org/10.3139/146.111696.

[37] J. Shen, M. Shi, B. Yan, H. Ma, N. Li, M. Ye, One-pot hydrothermal synthesis of Ag-reduced graphene oxide composite with ionic liquid, Journal of Materials Chemistry, 21, (2011) 7795–7801, https://doi.org/10.1039/c1jm10671f.

[38] J. Lu, J. Yang, J. Wang, A. Lim, S. Wang, K.P. Loh, One-pot synthesis of fluorescent carbon nanoribbons, nanoparticles, and graphene by the exfoliation of graphite in ionic liquids, ACS Nano, 3, 8, (2009) 2367–2375. https://doi.org /10.1021/nn900546b.

[39] N.S. Singh, L. Kumar, A. Kumar, S. Vaisakh, S.D. Singh, K. Sisodiya, S. Srivastava, M. Kansal, S. Rawat, Fabrication of zinc oxide/ polyaniline (ZnO/PANI) heterojunction and its characterisation at room temperature, Materials Science SemicondoctorProcessing, 60, (2017) 29–33. https://doi.org/0.1016/j.mssp.2016.12. 021.

[40] J. Stejskal, I. Sapurina, M. Trchová, Polyaniline nanostructures and the role of aniline oligomers in their formation, Prog. Polym. Sci, 35, Issue 12, (2010) 1420-1481. https://doi.org/10.1016 /j.progpolymsci.2010.07.006.

[41] M.L. Moreira, E.C. Paris, G.S. do Nascimento, V.M. Longo, J.R. Sambrano, V.R. Mastelaro, M.I.B. Bernardi, J. Andres, J.A. Varela, E. Longo, Structural and optical properties of CaTiO3 perovskite-based materials obtained by microwave assisted hydrothermal synthesis: An experimental and theoretical insight, ActaMaterialia, 57, Issue 17, (2009) 5174–5185.https://doi.org/10.1016 /j.actamat.2009.07.019.

[42] E.A.V. Ferri, T.M. Mazzo, V.M. Longo, E. Moraes, P.S. Pizani, M.S. Li, J.W.M. Espinosa, J.A Varela, E. Longo, Very intense distinct blue and red photoluminescence emission in MgTiO3 thin films prepared by the polymeric precursor method: An experimental and theoretical approach, The Journal of Physical Chemistry C, 116, 29, (2012) 15557–15567.https://doi.org/10.1021/jp30215 35.

[43] N. Roy, A. Roy, Growth and temperature dependent photoluminescence characteristics of ZnO tetrapods, Ceramics International, 41, Issue 3, Part A, (2015) 4154– 4160. https://doi.org/10.1016/j. ceramint.2014.11.113.

[44] A. Kushwaha, M. Aslam, Defect induced high photocurrent in solution grown vertically aligned ZnO nanowire array films, Journalof Applied Physics, 112, Issue 5, (2012) 054316. https://doi.org/10.1063/1.4749808.